Agricultural and Forest Meteorology 262 (2018) 81–88

Contents lists available at ScienceDirect

Agricultural and Forest Meteorology

journal homepage: www.elsevier.com/locate/agrformet

Microbial properties regulate spatial variation in the differences in heterotrophic respiration and its temperature sensitivity between primary and secondary forests from tropical to cold-temperate zones

Qing Wang[a], Nianpeng He[b,c,d,*], Li Xu[b], Xuhui Zhou[a]

[a] School of Ecological and Environmental Science, East China Normal University, Shanghai, 200241, China
[b] Key Laboratory of Ecosystem Network Observation and Modeling, Institute of Geographic Sciences and Natural Resources Research, Chinese Academy of Sciences, Beijing, 100101, China
[c] College of Resources and Environment, University of Chinese Academy of Sciences, Beijing 100049, China
[d] Institute of Grassland Science, Northeast Normal University, Key Laboratory of Vegetation Ecology, Ministry of Education, Changchun 130024, China

ARTICLE INFO

Keywords:
Forest
Incubation
Microbe
Soil respiration
Substrate
Temperature sensitivity

ABSTRACT

Large quantities of forest products globally have been lumbered, resulting in widespread conversion from primary forests [PFs] to secondary forests [SFs]. This transformation has exerted important impacts on the global carbon [C] cycle. Therefore, it is essential to clarify how soil C, which is a vital component of the global C pool, responds to the converting of forests from PFs to SFs, in parallel to identifying the underlying mechanisms. Here, nine paired (PFs and SFs) soil samples (0–10 cm) were obtained from tropical to cold-temperate zones along the north-south transect of eastern China (NSTEC). The heterotrophic respiration rate [R_H] as per soil organic C at a reference temperature of 20 °C [$R_{20\text{-}C}$] and its temperature sensitivity [Q_{10}] were measured and calculated through 14 d incubation experiments. Our results showed that most of $R_{20\text{-}C}$ and Q_{10} in SFs were greater than those in PFs. Strong spatial variation in the differences in $R_{20\text{-}C}$ and Q_{10} between PFs and SFs [$\triangle R_{20\text{-}C}$, $\triangle Q_{10}$] was observed along the NSTEC, with the greatest $\triangle R_{20\text{-}C}$, $\triangle Q_{10}$ being detected in the soils of mid-latitude forests. Overall, 83.2% of the spatial variation in $\triangle R_{20\text{-}C}$ was explained by physical-chemical and microbial properties, which contributed 68.5% and 52.4% variation solely, respectively. Similarly, 79% of the variation in $\triangle Q_{10}$ between PFs and SFs was explained by microbial properties, physical-chemical properties, and dissolved organic C, which contributed 81.6%, 10.5%, and 9% variation solely, respectively. Overall, our findings demonstrate high spatial variation in $\triangle R_H$ and $\triangle Q_{10}$ between PFs and SFs, which was mainly explained by microbial properties of soils.

1. Introduction

Forest ecosystems exchange energy, water, nutrients and, in particular, carbon [C] with the surrounding environment, and play major roles in the global C cycle. For instance, forests store large quantities of soil organic carbon [SOC] with high productivity (Battle et al., 2000; Goodale et al., 2002; Fang et al., 2007; He et al., 2017). Soil respiration [R_S] releases as much as half the total CO_2 production (Schlesinger and Andrews, 2000), most of which is produced by the activity of heterotrophic microorganisms [R_H] (Pries et al., 2017).

However, R_S in forest ecosystems is sensitive to changes in the climate and vegetation type, especially forest degradation, such as that primary forests [PFs] are converted to secondary forests [SFs] (Medlyn et al., 2005; Anderson-Teixeira et al., 2016). For example, SFs in the Amazon release more C (with *ca.* 1.3 Pg C yr^{-1}) than PFs (Espirito-Santo et al., 2014). However, Sheng et al. (2010) reported that the annual accumulation of R_S was reduced by 32% after converting PFs to SFs in a subtropical region. That is, converting PFs to SFs plays an important role to the global C pool, with controversy existing over how it influences the balance of C stocks. Because of human interventions associated with forest management and silviculture, two thirds of global PFs have been converted to SFs (FAO, 2006; Lungo et al., 2006), leading to a significant decrease in the soil C pool based on global meta-analysis (Don et al., 2011; Zhou et al., 2018). Therefore, it is important to clarify the mechanism leading to differences in *Rs* [$\triangle Rs$] as a result of converting PFs to SFs.

Based on existed researches, three properties could potentially explain spatial variation in $\triangle R_S$: microbial, substrate, and soil physical-

* Corresponding author.
E-mail address: henp@igsnrr.ac.cn (N. He).

https://doi.org/10.1016/j.agrformet.2018.07.007
Received 15 November 2017; Received in revised form 3 July 2018; Accepted 4 July 2018
Available online 09 July 2018
0168-1923/

chemical properties (Adachi et al., 2006; Zhang et al., 2016; Buchkowski et al., 2017). Usually, microbial properties included community composition, biomass, and activities of enzymes for C decomposition. Different microbes showed different preferences to soil organic matter [SOM]; for instance, bacteria prefer labile SOM, while fungi prefer recalcitrant SOM (Lehmann and Kleber, 2015). Thus, this difference in *Rs* might due to the various extracellular enzymes produced by microbes (Dungait et al., 2012; Ali et al., 2018). Previous studies reported that soil microbial biomass dominates the amount of enzymes present (Bååth, 1998; Fritze et al., 2000). Besides, enzyme activity might be regulated by pH (Min et al., 2014) and electricity conductivity (Iwai et al., 2012), which primarily influence microbial biomass. In addition to these physical-chemical properties, the growth of microorganisms could be significantly accelerated when available substrate is abundant, whereas an increase in the growth of microbes might result in a decrease in available substrate. That is, there existed an interaction effect between microbes and substrate to influence *Rs*. In particular, SOM quality might change the temperature sensitivity [Q_{10}] of *Rs*, which is closely related to the "Carbon quality –temperature sensitivity" hypothesis (Bosatta and Ågren, 1999). That is, substrates of low quality require higher energy for microbes to degrade, leading microbes to exhibit higher sensitivity to warming than they would in substrates of high quality (Gershenson et al., 2009; He et al., 2013; Wang et al., 2016b).

Nevertheless, previous studies generally focused on single research sites, making it difficult to obtain a general pattern and elucidate the underlying mechanisms driving $\triangle R_S$, particularly in China (Sheng et al., 2010; Liu et al., 2011; Shi et al., 2015). Forests in China extend across most of forest types in the Northern Hemisphere (18.74–53 °N) and exhibit a significant hydrothermal gradient (Zhang and Yang, 1995). Due to the rapid growth in the economy and increased demand for timber and food production, deforestation increased at a sharp rate in China during the second half of the 20th century, resulting in a large amount of PFs being converted to SFs (Shi et al., 2009). Therefore, understanding the pattern of $\triangle R_S$ in China might help us to elucidate how forest degradation affects soil C stocks at regional or global scales.

In this study, we collected nine paired (PFs *vs.* SFs) surface (0–10 cm) forest soils along the north-south transect of eastern China [NSTEC]. Then, we conducted a 14-d incubation experiment to investigate differences in heterotrophic respiration rate (per soil organic C at a reference temperature of 20 °C [$R_{20\text{-}C}$]) and Q_{10} between PFs and SFs ($\triangle R_{20\text{-}C}$, $\triangle Q_{10}$), along with differences in the background values of potential explanatory factors (physical-chemical *vs.* substrate *vs.* microbial properties). We aimed to clarify: 1) whether R_H in SFs are consistently higher than that in PFs; 2) whether a clear spatial trend in $\triangle R_H$ ($\triangle R_{20\text{-}C}$, $\triangle Q_{10}$) exists from tropical to cold-temperate zone; and 3) what factors dominate the spatial variation in $\triangle R_H$ ($\triangle R_{20\text{-}C}$, $\triangle Q_{10}$)?

2. Materials and methods

2.1. Sites description and pre-treatment

The NSTEC (108.86°–123.29 °W, 18.74°–51.76 °N) is a unique forest belt (Fig. 1) that has a significant thermal gradient (Zhang and Yang, 1995; Zhao et al., 2016) from north to south. The mean annual temperature ranges from –3.67 °C to 23.15 °C and the mean annual precipitation ranges from 473 mm to 2266 mm (Table 1). Nine coupled forests with relatively homogenous and representative vegetation were selected along the NSTEC. They were designated as cold-temperate coniferous forest (site: Huzhong), temperate *Pinus koraiensis*-broadleaf mixed forest (Liangshui and Changbai), warm temperate deciduous broad-leaved forest (Dongling and Taiyue), north subtropical evergreen and deciduous broad-leaved mixed forest (Shennong), subtropical evergreen broad-leaved forest (Jiulian), south subtropical evergreen broadleaved forest (Dinghu), and tropical mountain rain forest (Jianfeng), respectively (Fig. 1, Table 1) (Tian et al., 2016a; Wang et al., 2016c). PFs were either long-term experimental sites or sites selected from natural protected areas in China, to exclude any strong human disturbance over the last five decades. SFs were located adjacent to PFs and had similar topography and slope with secondary succession following lumber harvesting.

Field sampling was conducted from July to August. We set up four 30 m × 40 m plots in each forest (He et al., 2018). Soil surface samples (0–10 cm) were collected from four randomly chosen locations in each plot and were combined to form one composite sample for per plot (Wang et al., 2016b; Xu et al., 2017). Soil samples were sieved (< 2 mm diameter), with all roots and visible organic debris being removed manually. For each forest, homogenized soils were divided into three subsamples: (1) froze at −80 °C to measure soil microbial properties, including enzyme activities and microbial community, (2) to measure soil biochemical and physical properties, and (3) stored at 4 °C before incubation experiments.

2.2. Analysis of soil physical-chemical and substrate properties

In this study, soil physical-chemical properties included soil pH, oxidation-reduction potential [ORP], conductivity [COND], bulk density [BD], and soil texture (Table S1). pH, oxidation-reduction potential, and conductivity were measured by "Ultrameter II" (Myron L Company, USA) (slurry of soil and ultrapure water, 1:2.5). Particle size distribution was determined using the Mastersizer 2000 (Malvern, UK) laser diffractometer (Sochan et al., 2012), and was further classified into clay (< 2 μm), silt (2–50 μm) and sand (50–2000 μm) based on the soil texture classification system of American.

Soil water content was measured using the methods of oven-dried and weighted. Soil water holding capacity was determined by rewetting it for 12 h, followed by draining it through filter paper for 12 h. Soil water content was calculated by the soil samples that were weighed before and after over-drying at 105 °C for 24 h (Wang et al., 2016b).

We measured four substrate properties, *i.e.*, the contents of SOC, total nitrogen [TN], dissolved organic carbon [DOC], and dissolved total nitrogen [DTN] (Table S2). The contents of SOC and TN were measured using an elemental analyzer (Elementar, Vario Max, Germany). DOC and DTN were measured using the non-fumigated samples (one part of chloroform-fumigation for microbial biomass) with a total organic carbon instrument (liquid TOC II, USA) and continuous flow analyzer (Futura, France), respectively.

2.3. Analysis of soil microbial properties

To assess how microbial properties affect $\triangle R_H$, we selected the microbial biomass, community structural, and enzymes related to C decomposition (Table S3). The chloroform-fumigation method was used to estimate microbial biomass, including microbial biomass C [MBC] (1/Kc = 2.22, Baumann et al., 1996) and microbial biomass nitrogen [MBN] (1/Kn = 1.85, Brookes et al., 1985), with 0.5 M K_2SO_4 (slurry of soil and K_2SO_4 solution, 1:5). The leach liquor was measured with a total organic C instrument (liquid TOC II; USA) and continuous flow analyzer (Futura, France), respectively (Wang et al., 2016b). Phospholipid fatty acid content was measured to obtain the microbial community structural using the mild alkaline methyl esterification method and gas chromatography and mass spectrometry (Thermo ISQ TRACE GC system Ultra ISQ, Germany) (Xu et al., 2015). Based on the results of phospholipid fatty acid and the rules of Frostegard and Bååth (1996), bacteria, fungi, actinomyces were classified as three different microbial communities.

The enzymes related to C decomposition selected in this study were based on previous studies (Xu et al., 2015; Min et al., 2014), and included β-D-glucosidase [βG, representing the terminal reaction in cellulose degradation], *N*-acetyl-β-D-glucosidase [NAG, representing hydrolyzes leucine and other hydrophobic amino acids from the N-

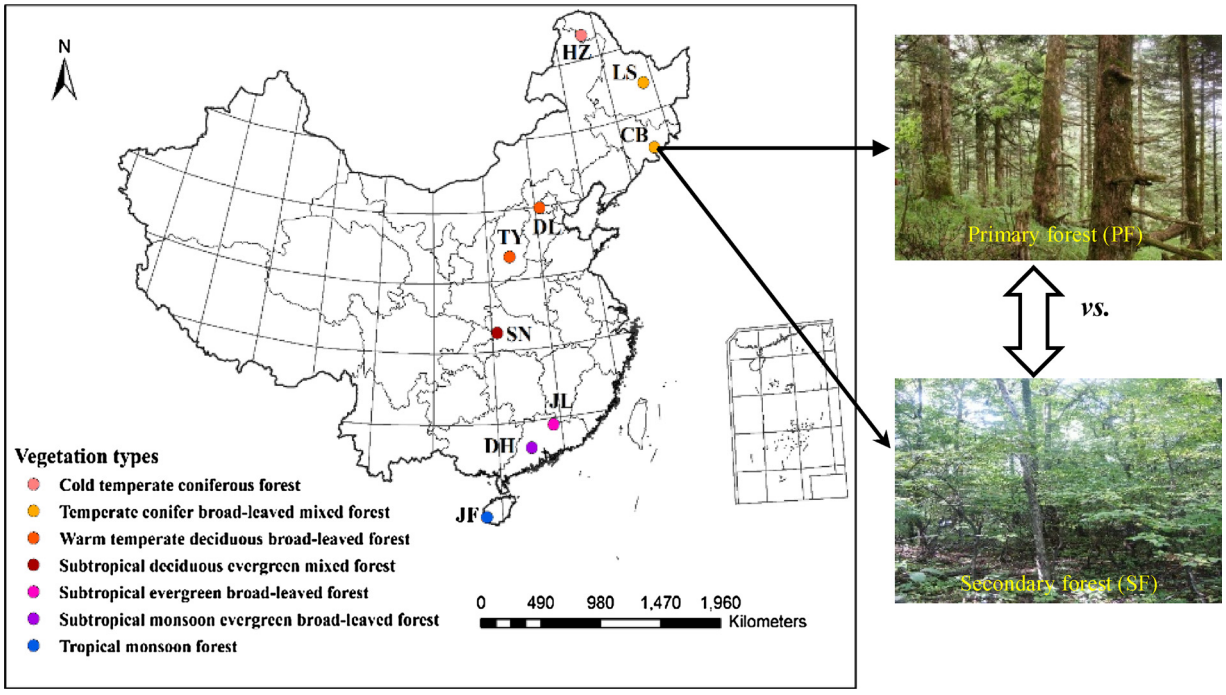

Fig. 1. Locations of the nine paired forests (primary forests *vs*. secondary forests) along the north-south transect of eastern China. Sites: HZ, Huzhong; LS, Liangshui; CB, Changbai; DL, Dongling; TY, Taiyue; SN, Shennong; JL, Jiulian; DH, Dinghu; JF, Jianfeng. The inserts are examples of primary forest (PFs) and secondary forest (SFs) at the CB site.

terminus of polypeptides], acid phosphatase [AP, representing hydrolyze phosphate esters including phosphomonoesters, phosphodiesters, and in some cases phosphosaccharides that release phosphate], leucine aminopeptidase [LAP, representing hydrolyzes leucine and other hydrophobic amino acids from the N-terminus of polypeptides]. The activities of βG, NAG, AP, and LAP were measured using the method of Saiya-Cork et al. (2002) with microplate fluorometer (SynergyH4 Hybrid Reader, SynergyH4 BioTek, USA). More details on the measurements of enzyme activity and microbial community are provided by Xu et al. (2015, 2017).

2.4. Design of incubation experiment

Soil sampling was conducted when the average daily temperature was approximately 20 °C along the NSTEC, ranging from a minimum of approximately 15 °C and a maximum of approximately 25 °C. Thus, 20 °C was used as the reference temperature for obtaining R_{20}, with an increase of 10 °C (from 15 °C to 25 °C) for obtaining Q_{10} (Leifeld and von Lutzow, 2014).

We set 12 replicates at each sample site, with four replicates at each sample site × three temperature treatments (R_{20} (20 °C) and Q_{10} (15 °C and 25 °C)) (Craine et al., 2010). We allotted the replicates to 40 g fresh soil at each sample site with 10 g of quartz sand (preventing soil from hardening) in a 150-ml polyethylene plastic bottle and we adjusted

Table 1
Basic soil properties at the sampled sites.

Sampling Sites	Longitude (E)	Latitude (N)	Altitude (m)	MAT[b] (ºC)	MAP (mm)	Vegetation types	Dominant species	Soil type
HZ[a]	123.29°	51.76°	850	–3.67	473	Cold–temperate coniferous forest	*Larix gmelinii* Rupr, *Pinus. Sylvestris* L., *Betula. Platyphylla* Suk.	Grey forest soil
LS	128.89°	47.18°	401	0.01	648	Temperate conifer broadleaf mixed forest	*L. gmelinii* Rupr, *P. koraiensis* Siebold, *B. platyphylla* Suk.	Dark brown soil
CB	128.09°	42.40°	758	2.79	691	Temperate conifer broadleaf mixed forest	*L. gmelinii* Rupr, *P. koraiensis* Siebold, *Quercus Mongolica* Fisch.	Dark brown soil
DL	115.48°	39.97°	972	6.55	539	Warm temperate deciduous broad–leaved forest	*P. tabulaeformis* Carr, *Q. wutaishanica* Mayr, *L. principis–rupprechtii* Mayr	Brown soil
TY	112.10°	36.68°	1668	5.98	644	Warm temperate deciduous broad–leaved forest	*Q. wutaishanica* Mayr, *P. tabulaeformis* Carr, *Populus. davidiana* Dode.	Cinnamon soil
SN	110.49°	31.32°	1510	8.50	1447	North subtropical evergreen deciduous mixed forest	*Fagus engleriana* Seemen, *Q. serrata* Thunb, *Cyclobalanopsis oxyodon* Oerst.	Yellow brown earth
JL	114.44°	24.57°	562	18.22	1770	Subtropical evergreen broad–leaved forest	*S. superb* Gardn, *Castanopsis. fabri* Hance, *C. carlesii* Hayata.	Red earth
DH	112.54°	23.17°	240	21.83	1927	South subtropical evergreen broad–leaved forest	*Schima. Superba* Gardn, *Cryptocarya. Chinensis* Hemsl, *P. massoniana* Lamb.	Laterite
JF	108.86°	18.74°	809	23.15	2266	Tropical mountain rainforest	*Schoepfia. Jasminodora* Sieb, *Ficus. vasculosa* Wall, *Madhuca. Hainanensis* Chun.	Lateritic yellow earth

[a] HZ, Huzhong; LS, Liangshui; CB, Changbai; DL, Dongling; TY, Taiyue; SN, Shennong; JL, Jiulian; DH, Dinghu; JF, Jianfeng.
[b] MAT, mean annual temperature; MAP, mean annual precipitation.

water content to 55% water holding capacity. In general, 55% of water holding capacity is the optimal water content for microbial activity (Gamboa and Galicia, 2011). All soil samples were first pre-incubated at 20 °C for 1 week and were then put into incubators set at 15 °C, 20 °C, and 25 °C, respectively. To maintain relatively stable soil moisture levels, soil water content was checked and adjusted every 3–4 d by weighting it. All samples were measured at day 0, 7 and 14 in the 14-d incubation experiment. The data for analyzing R_{20} and Q_{10} was the mean value of heterotrophic respiration rate based on three independent measurements. R_H was synchronously monitored with an automatic control temperature-soil flux system (PRI-8800; PRE-ECO, Beijing, China), which was newly developed as a modification of He et al. (2013).

2.5. Data analyses

Soil heterotrophic respiration rates were calculated as the slope of changed CO_2 concentration with conversion factors as follows (Eq. (1): He and Yu, 2016; Wang et al., 2016b; Li et al., 2017; Liu et al., 2017):

$$R_H = \frac{C \times V \times \alpha \times \beta}{m} \quad (1)$$

where R_H is the soil heterotrophic respiration rate (μg C g^{-1} soil d^{-1}); C is the slope of change in CO_2 concentration (ppm); V is the volume of the incubation bottle and gas tube (m^{-3}); m is the soil mass (g); α is the conversion coefficient of CO_2 mass (translate the volume of CO_2 to the mass of CO_2-C); and β is a conversion coefficient of time (translating the time from second to day).

To assess the effect of SOC content on R_H, we calculated R_{20} based on SOC content ($R_{20\text{-}C}$, μg C g SOC^{-1} d^{-1}), following some previous studies (Shi and Marschner, 2014; Wang et al., 2016a; Ali et al., 2018):

$$R_{20-C} = \frac{R_{20}}{C} \quad (2)$$

where C is the SOC content (%).

Q_{10} is calculated as Eq. (3) (Thiessen et al., 2013):

$$Q_{10} = \left(\frac{R_{25}}{R_{15}}\right)^{\frac{10}{T_{25}-T_{15}}} \quad (3)$$

where R_{25} and R_{15} are the heterotrophic respiration rates at high temperature (T_{25}) and low temperature (T_{15}), respectively.

We also calculated two indexes to characterize differences in R_H caused by conversion from PFs to SFs as the following equations:

$$\Delta R_{20-C} = \frac{R_{20-C}(PF_i)}{R_{20-C}(SF_i)} \quad (4)$$

$$\Delta Q_{10} = \frac{Q_{10}(PF_i)}{Q_{10}(SF_i)} \quad (5)$$

where i is sample site (Huzhong, Liangshui, Changbai, Dongling, Taiyue, Shennong, Jiulian, Dinghu, Jianfeng, respectively).

2.6. Statistical analysis

A bubble diagram was created to display the relationships of soil physical-chemical, substrate, microbial, and R_H properties with latitude and altitude (or mean annual temperature and precipitation). An independent-sample t-test was conducted to test the differences in $R_{20\text{-}C}$ and Q_{10} between PFs and SFs along the NSTEC. Pearson's correlations among soil physical-chemical, substrate, microbial, and R_H properties were conducted using the Rstudio 3.4.3. Furthermore, we assessed and transferred the nonlinear relationships between soil physical-chemical, substrate, microbial and R_H properties into linear forms using general addition models with Rstudio 3.4.3 (Table S4). All of the linear influencing factors were then subjected to stepwise regression, to select the significant factors driving $\triangle R_H$ using SPSS 18.0 for Windows (SPSS Inc., Chicago, IL, USA). The significance level was set at $P = 0.05$.

The significant influencing factors selected by stepwise regression were used in the redundancy analysis using Canoco 5.0 (ter Braak and Smilauer, 2012) to explore the contributions of soil physical-chemical, substrate, and microbial properties to $\triangle R_H$. Because the redundancy analysis is not able to provide causal relationships among multiple interactional variables explicitly, we used structural equation models to determine the contribution of each physical-chemical, substrate, and microbial property to $\triangle R_H$ using Amos 7 for Windows (IBM, Chicago, IL, USA). The results of structural equation modeling were evaluated with the Chi square test, root mean square error of approximation, and the goodness-of-fit statistic (Hooper et al., 2008; Flores-Rentería et al., 2016).

3. Results

3.1. Differences in soil properties between PFs and SFs along the NSTEC

Only the differences of LAP, bacteria, and actinomyces between PFs and SFs showed clear linear trends with changes in climate, decreasing with increasing mean annual temperature and precipitation along the NSTEC (Fig. 2). That is, differences of LAP, bacteria and actinomyces between PFs and SFs were greater in the cold and dry zone compared to the hot and wet zone.

3.2. Changes to $R_{20\text{-}C}$ and Q_{10} along the NSTEC

$R_{20\text{-}C}$ differed significantly among the nine coupled forests along the NSTEC ($P < 0.001$) and the greatest differences in $R_{20\text{-}C}$ between PFs and SFs occurred in the mid-latitudes (31.3–39.9 °N, Fig. 3). The Q_{10} values in the nine coupled forests along the NSTEC were approximately 1–2, except for the Q_{10} of SF in site of Taiyue (2.84, 36.7 °N) (Fig. 3), with a mean Q_{10} value of 1.49. The Q_{10} values were significantly higher in SFs compared to PFs in the mid-latitudes (31.3–39.9 °N, $P < 0.05$).

$\triangle R_{20\text{-}C}$ at low latitudes with high altitude and high latitudes with low altitude was higher than that in the other zones to some extent (Fig. 4). $\triangle Q_{10}$ showed a quadratically trend with latitude and altitude (Fig. 4).

The area of the circle represents the magnitude of the mean ratios in the heterotrophic respiration rate per soil organic carbon at 20 °C ($R_{20\text{-}C}$) and temperature sensitivity (Q_{10}) (primary forest *vs.* secondary forest).

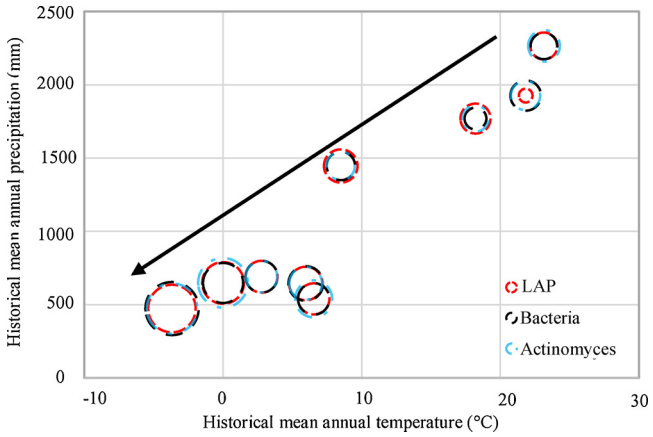

Fig. 2. Changes in the mean ratios of LAP, bacteria, and actinomyces between primary forest and secondary forest with mean annual temperature (°C) and precipitation (mm).
The area of the circle represents the size of the mean ratios of leucine aminopeptidase (LAP), bacteria, and actinomyces between primary forest and secondary forest, respectively.

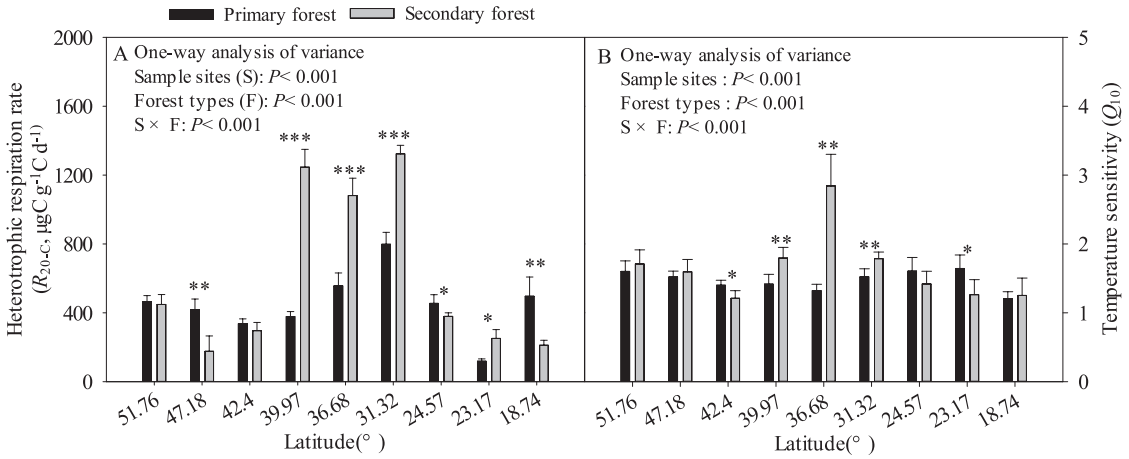

Fig. 3. Mean values of the heterotrophic respiration rate per soil organic carbon at 20 °C ($R_{20\text{-}C}$) and temperature sensitivity (Q_{10}) along the latitudinal gradient. Data are presented as means and standard deviation (n = 4). An independent-sample *t*-test was conducted to test the differences between each pair of primary and secondary forest types. *, **, *** represent significant differences at $P < 0.05$, $P < 0.01$, and $P < 0.001$, respectively.

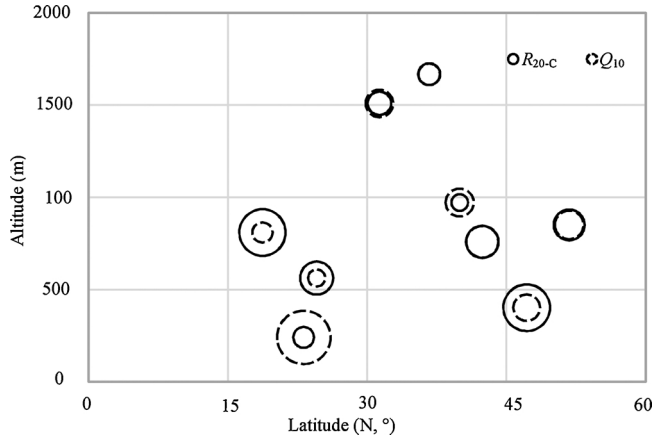

Fig. 4. Mean ratios in the heterotrophic respiration rate per soil organic carbon at 20 °C ($R_{20\text{-}C}$) and temperature sensitivity (Q_{10}) (primary forest *vs.* secondary forest) with respect to latitudinal and altitudinal gradient.

3.3. *Factors driving spatial variation in* $\triangle R_{20\text{-}C}$ *and* $\triangle Q_{10}$

$\triangle R_{20\text{-}C}$ was significantly and positively related to COND and pH (Fig. 5). In comparison, $\triangle Q_{10}$ was significantly related to the content of MBC, ORP, and the activities of βG, AP, and LAP. Specifically, pH has an important positive effect on content of DTN, fungi, bacteria, actinomyces, and LAP (Fig. 5). βG and NAG changed significantly and positively with ORP and COND. Overall, stepwise regression analysis demonstrated that the dominant factors driving spatial variation in $\triangle R_{20\text{-}C}$ were physical-chemical (pH, BD) and microbial (bacteria, MBC, βG, and NAG) factors. In comparison, physical-chemical (pH, clay), substrate (DOC), and microbial (bacteria, MBC and LAP) properties were the dominant factors driving spatial variation in $\triangle Q_{10}$ (Table S5).

The values of the correlation coefficients are indicated by the scale bar. Physical-chemical properties included: pH, silt, clay, sand, COND (conductivity), ORP (oxidation reduction potential), BD (bulk density); substrate properties included: TN (total nitrogen), DOC (dissolved organic carbon), DTN (dissolved total carbon); microbial properties included: fungi, bacteria, actinomyces, βG (β-D-Glucosidase), NAG (*N*-acetyl-β-D-glucosidase), AP (acid phosphatase), LAP (leucine aminopeptidase); heterotrophic respiration properties included: $R_{20\text{-}C}$ (heterotrophic respiration at a reference temperature of 20 °C), Q_{10} (sensitivity of heterotrophic respiration to temperature). All of the data for this analysis were the mean ratios of values between primary and secondary forests. *, **, and *** represent significant differences at

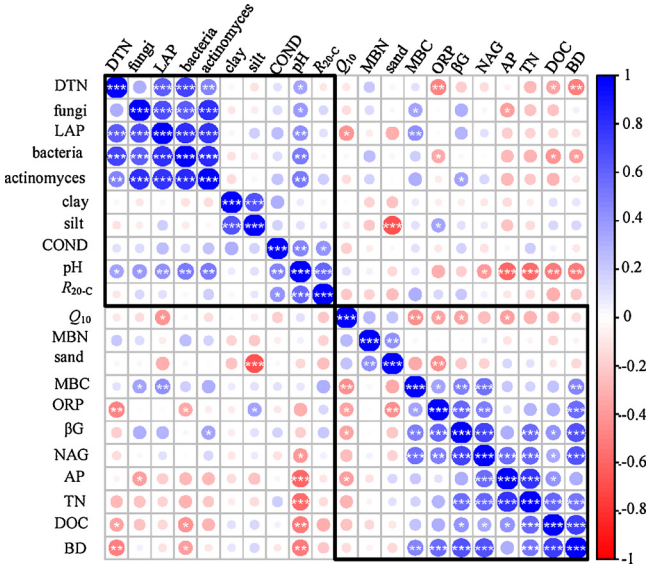

Fig. 5. Pearson's correlations among soil physical-chemical, substrate, microbial, and heterotrophic respiration properties.

$P < 0.05$, $P < 0.01$, and $P < 0.001$, respectively.

Redundancy analysis showed that 83.2% of spatial variation in $\triangle R_{20\text{-}C}$ was explained by those factors selected by the stepwise regression analysis. Specifically, physical-chemical and microbial properties explained 52.4% and 68.5% of variation in $\triangle R_{20\text{-}C}$ respectively, with a negative interaction effect (–37.7%) (Fig. 6 A). Overall, 79% of spatial variation in $\triangle Q_{10}$ along the NSTEC was explained by the factors selected in the stepwise regression analysis. Specifically, microbial, physical-chemical, and substrate properties explained 81.6%, 10.5% and 9% of spatial variation in $\triangle Q_{10}$ (Fig. 6B), respectively, with negative interaction effects on each other.

Factors that explained "differences in $R_{20\text{-}C}$ between primary and secondary forests" included physical-chemical (pH, bulk density), microbial properties (bacteria, microbial biomass carbon (MBC), activity of *N*-acetyl-β-D-glucosidase and β-D-Glucosidase). Factors that explained "differences in Q_{10} in between primary and secondary forests" included substrate (DOC), physical-chemical (content of clay and pH), microbial properties (MBC, bacteria and activity of leucine aminopeptidase (LAP)). All of the data for this analysis were based on the step-wise regression analysis from all physical-chemical, substrate, and microbial properties (Table S5). **, represent significant differences at

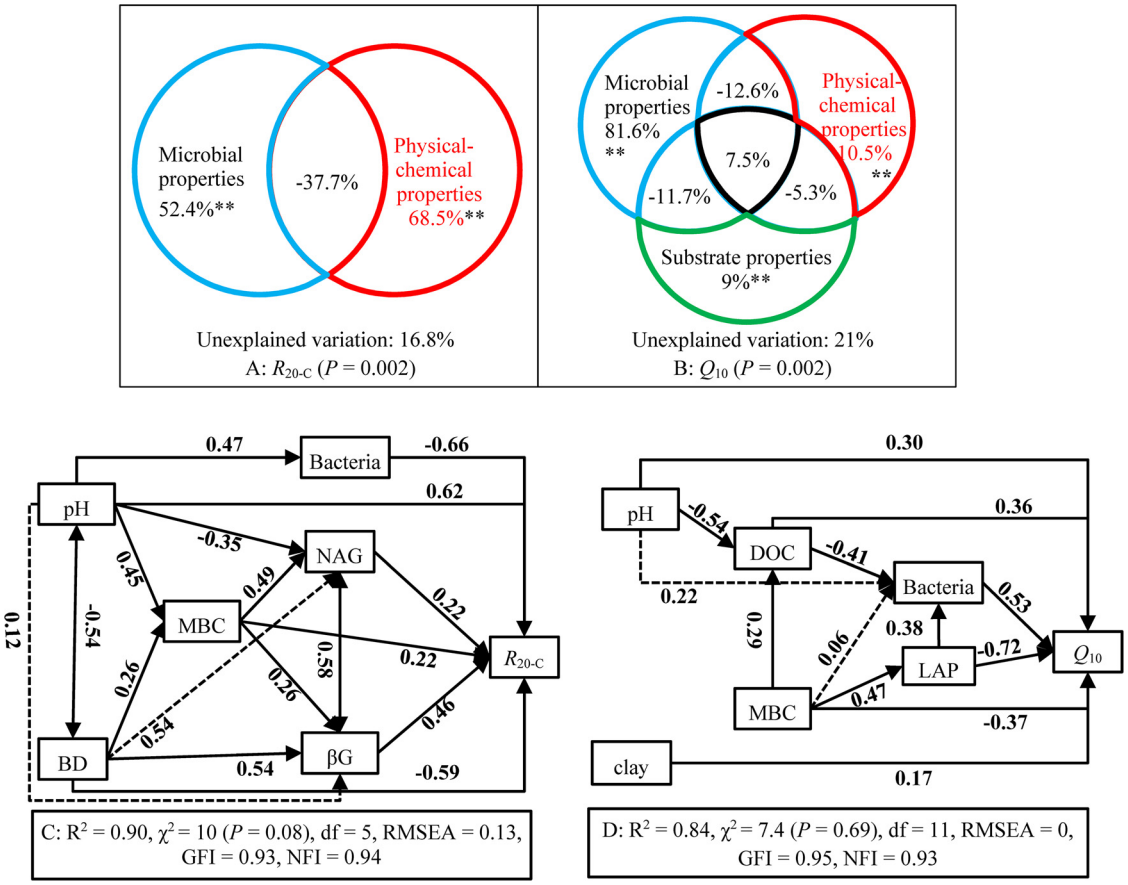

Fig. 6. Redundancy analysis and structural equation models of the direct and indirect effects of the factors influencing the differences in the ratios of $R_{20\text{-}C}$ (heterotrophic respiration rate per g soil organic carbon at 20 °C, A, C) and Q_{10} (temperature sensitive, B, D) between primary and secondary forests.

$P < 0.01$. Solid line represents the direct effect and dashed line represents the indirect effect. All of the relationships for structural equation models showed here were significant. RMSEA: root mean square error of approximation; GFI: goodness of fit index; NFI: normed fit index.

Similarly, structural equation modeling demonstrated that the factors selected by stepwise regression analysis explained 90% of spatial variation in $\triangle R_{20\text{-}C}$ (Fig. 6 C) and 84% of that in $\triangle Q_{10}$ (Fig. 6 D). Bacteria and βG were the main microbial factors and had opposing effects on the variation in $\triangle R_{20\text{-}C}$. pH and BD were the main physical-chemical factors and had opposing effects on variation in $\triangle R_{20\text{-}C}$. In comparison, bacteria and LAP, as well as DOC and MBC, had direct and opposite effects on variation in $\triangle Q_{10}$. Clay had only a positive direct effect on variation in $\triangle Q_{10}$.

4. Discussions

4.1. *Strong spatial variation in $^{\triangle}R_H$ from tropical to cold-temperate zones*

Although the mean value of $\triangle R_{20\text{-}C}$ was lower than 1, the $R_{20\text{-}C}$ and Q_{10} of SFs were not always significantly higher than the values documented in PFs. Some results at individual sites were consistent with that of Shi et al. (2009), while the mean effect of converting forest on R_H was antagonistic to the meta-analyses of global data (Zhou et al., 2018). An exception to Q_{10} at the latitude of 24.6 °N was also detected in the study of Sheng et al. (2010), who found that Q_{10} increased from 2.10 in PFs to 2.71 in SFs, whereas the annual R_S declined by 32% following the conversion of PFs to SFs. Considering the strong spatial variation in R_H among PFs and SFs (Liu et al., 2017), it might not be appropriate to use the mean value of R_H in the C model to assess the global C dynamics.

4.2. *Microbial and physical-chemical properties jointly drive spatial variation in $^{\triangle}R_{20\text{-}C}$*

Variation in soil properties after forest conversion mainly reflected in soil microbial activity (Blagodatskaya et al., 2016), soil temperature (Garten et al., 1999; Niklinska and Klimek, 2007), precipitation, conductivity (Smith et al., 2002), and pH (Smith et al., 2002), as well as soil nutrient (Tian et al., 2016b). In the current study, we controlled soil samples under 55% water holding capacity, which made it independent of soil moisture, and we calculated the R_H based on a specific unit (g^{-1} SOC^{-1}), which was independent of SOC content. Therefore, the effects of soil moisture and SOC content on $\triangle R_{20\text{-}C}$ were not considered here (Ali et al., 2018).

Excluding SOC and soil moisture, large spatial variation in $\triangle R_{20\text{-}C}$ from tropical to cold-temperate zones was attributed to spatial variation in soil microbial (βG, NAG, and bacteria) and physical-chemical (pH and BD) properties, with significant negative interaction. The direct effects of microbial properties on $R_{20\text{-}C}$ here have been supported by Xu et al. (2015), especially for some studies of other transects (Colman and Schimel, 2013; Ali et al., 2018). In contrast to the meta-analyses at the global scale (Zhou et al., 2018), we found that converting PFs to SFs increased microbial composition as a whole, including bacteria and fungi. Of note, enzyme activity was the main factor driving spatial variation in R_H (Fig. 6), showing a decreasing trend with increasing annual mean temperature and precipitation (Fig. 2). The importance of enzyme activity (Table S5) was supported by Xu et al. (2015), who found that R_H shows a significant positive relationship with soil enzyme

activity. Furthermore, the activities of enzymes responsible for SOC decomposition was closely related to that for nitrogen decomposition (Fig. 5). Overall, our results supported a currently hot issue about whether these effects of microbial properties on R_H should be incorporated into C model (Wieder et al., 2015; Huang et al., 2018), especially the interaction of enzymes for C and nitrogen decomposition.

In addition to microbial properties, physical-chemical properties play crucial roles in the spatial variation of $\triangle R_{20\text{-}C}$. Xu et al. (2016) previously reported that the spatial patterns of soil respiration are regulated by biological and physical-chemical variables jointly. Usually, soil with lower BD has more interspace, facilitating microbes by providing greater access to water, oxygen, and substrate (Kaiser et al., 2015). Thus, higher BD leads to greater soil compaction (Sohng et al., 2017), which decreases access to water and oxygen by microbes, and might explain the negative effect of BD on $\triangle R_{20\text{-}C}$ to some extent.

Of note, pH and BD had opposite effects on the spatial variation of $\triangle R_{20\text{-}C}$. Usually, pH affects mineral-mineral or organo-mineral interactions (Kaiser et al., 2015), which then influence BD. The spatial variation in the difference in pH between PFs and SFs observed in the current study was similar to that observed by Hong et al. (2018). Furthermore, pH played an important role in connecting physical-chemical and microbial properties (Chen et al., 2016). Specifically, variation in COND, DTN, fungi, and actinomycetes was significantly positively related to that of pH, which have been verified other studies (Shen et al., 2013; Xiong et al., 2012). The positive and indirect effects of pH on the enzyme activities of NAG and βG has also been documented by previous studies (Bååth, 1998; Fritze et al., 2000).

4.3. *Microbial properties drive spatial variation in* $\triangle Q_{10}$

The direct effects of microbial properties (bacteria, LAP, and MBC), accompanied with the direct and indirect effects of physical-chemical properties (pH and clay) and DOC, regulated spatial variation in $\triangle Q_{10}$. LAP is the most important microbial factor, and had a significantly negative effect on spatial variation in $\triangle Q_{10}$. Besides, $\triangle Q_{10}$ decreased with increasing differences in MBC between PFs and SFs (Fig. 5). This similar effects of LAP and MBC on $\triangle Q_{10}$ was also reported by Baldrian (2014), who found that variation in microbial biomass shapes the distribution of enzymes at large spatial scales. Of course, variations resulted from changes in dominant vegetation, land use type, and soil physicochemical properties also played important roles in the correlation between LAP and MBC. Furthermore, the dominant microbial factors for $\triangle Q_{10}$ have a close coupling relationship with the nitrogen cycle, similar to that for $\triangle R_{20\text{-}C}$. This coupling might be regulated by a stable stoichiometric ratio of C: N for microbial metabolism (Sinsabaugh et al., 2008; Sharon and Ford, 2013).

Similar to $\triangle R_{20\text{-}C}$, pH also acts as the crucial physical-chemical factor in combination with substrate and microbial properties, and played a positive and direct effect on $\triangle Q_{10}$ (Ali et al., 2018). pH could change the sensitivity of enzymes for C decomposition to temperature (Min et al., 2014), which eventually causes $\triangle Q_{10}$ to change.

In the current study, DOC had a significant positive effect on variation in $\triangle Q_{10}$ (Fig. 6). This effect is explained by the "Carbon quality-temperature sensitivity" hypothesis (Bosatta and Ågren, 1999). In general, DOC is labile substrate and is important for the metabolism of microbes (Fang et al., 2005). The observed relationships between Q_{10} and DOC demonstrated that the hypothesis could not be verified for PFs but could be verified for SFs (Fig S1). This differences implies that PFs have similar substrate quality at a spatial scale, however, converting forests might break this homogeneity, which is shaped by spatial heterogeneity. Thus, the weak variation in Q_{10} at the both ends of the latitudinal range have similar amounts of DOC for PFs and SFs (Fig. 3). That is, soils with less DOC might consume available DOC quickly and then consume recalcitrant SOM, leading to higher Q_{10} compared to soils with enough available substrate. This processes might produce greater $\triangle Q_{10}$, especially in mid-latitude forests.

5. Conclusions

We explored spatial variation in $\triangle R_{20\text{-}C}$ and $\triangle Q_{10}$ in relation to differences in the background conditions of physical-chemical, substrate, and microbial factors in the nine paired forest soils (PFs *vs*. SFs) from tropical to cold temperate zones. Converting forests from PFs to SFS does not always result in more C loss. There was strong spatial variation in $\triangle R_H$ along the NSTEC, especially in the mid-latitudes. Variation in $\triangle R_{20\text{-}C}$ was mainly attributed to variation in the differences in pH, BD, bacteria, MBC, βG, and NAG, whereas variation in $\triangle Q_{10}$ was mainly attributed to variation in the differences in MBC, LAP, bacteria, clay, pH and DOC. Overall, our findings demonstrate that microbial properties are dominant factors explaining spatial variation in the differences in $\triangle R_{20\text{-}C}$ and Q_{10} between PFs and SFs.

Data accessibility

Data share can be contacted with Dr. N. P. He (E-mail: henp@igsnrr.ac.cn)

There are no conflicts of interest to declare.

Acknowledgements

Funding for this work came from the National Key R&D Program of China (2017YFC0503904, 2016YFC0500102), from the Natural Science Foundation of China (41571130043, 31770655), and from the Program of Youth Innovation Research Team Project (LENOM2016Q0005). We thank the anonymous reviewers for improving this MS.

Appendix A. Supplementary data

Supplementary material related to this article can be found, in the online version, at doi:https://doi.org/10.1016/j.agrformet.2018.07.007.

References

Adachi, M., Bekku, Y.S., Rashidah, W., Okuda, T., Koizumi, H., 2006. Differences in soil respiration between different tropical ecosystems. Appl. Soil Ecol. 34, 258–265.
Ali, R.S., Kandeler, E., Marhan, S., Demyan, M.S., Ingwersen, J., Mirzaeitalarposhti, R., Rasche, F., Cadisch, G., Poll, C., 2018. Controls on microbially regulated soil organic carbon decomposition at the regional scale. Soil Biol. Biochem. 118, 59–68.
Anderson-Teixeira, K.J., Wang, M.M.H., McGarvey, J.C., LeBauer, D.S., 2016. Carbon dynamics of mature and regrowth tropical forests derived from a pantropical database (TropForC-db). Global Change Biol. 22, 1690–1709.
Bååth, E., 1998. Growth rates of bacterial communities in soils at varying pH: a comparison of the thymidine and leucine incorporation techniques. Microb. Ecol. 36, 316–327.
Baldrian, P., 2014. Distribution of extracellular enzymes in soils: spatial heterogeneity and determining factors at various scales. Soil Sci. Soc. Am. J. 78, 11–18.
Battle, M., Bender, M.L., Tans, P.P., White, J.W.C., Ellis, J.T., Conway, T., Francey, R.J., 2000. Global carbon sinks and their variability inferred from atmospheric O_2 and delta C-13. Science 287, 2467–2470.
Baumann, A., Schimmack, W., Steindl, H., Bunzl, K., 1996. Association of fallout radiocesium with soil constituents: effect of sterilization of forest soils by fumigation with chloroform. Radiat. Environ. Biophys. 35, 229–233.
Blagodatskaya, E., Blagodatsky, S., Khomyakov, N., Myachina, O., Kuzyakov, Y., 2016. Temperature sensitivity and enzymatic mechanisms of soil organic matter decomposition along an altitudinal gradient on Mount Kilimanjaro. Sci. Rep. 6. https://doi.org/10.1038/srep22240.
Bosatta, E., Ågren, G.I., 1999. Soil organic matter quality interpreted thermodynamically. Soil Biol. Biochem. 31, 1889–1891.
Brookes, P.C., Kragt, J.F., Powlson, D.S., Jenkinson, D.S., 1985. Chloroform fumigation and the release of soil nitrogen: the effects of fumigation time and temperature. Soil Biol. Biochem. 17, 831–835.
Buchkowski, R.W., Bradford, M.A., Grandy, A.S., Schmitz, O.J., Wieder, W.R., 2017. Applying population and community ecology theory to advance understanding of belowground biogeochemistry. Ecol. Lett. 20, 231–245.
Chen, L.Y., Liang, J.Y., Qin, S.Q., Liu, L., Fang, K., Xu, Y.P., Ding, J.Z., Li, F., Luo, Y.Q., Yang, Y.H., 2016. Determinants of carbon release from the active layer and permafrost deposits on the Tibetan Plateau. Nat. Commun. 7.
Colman, B.P., Schimel, J.P., 2013. Drivers of microbial respiration and net N mineralizationat the continental scale. Soil Biol. Biochem. 60, 65–76.
Craine, J.M., Fierer, N., McLauchlan, K.K., 2010. Widespread coupling between the rate and temperature sensitivity of organic matter decay. Nat. Geosci. 3, 854–857.
Don, A., Schumacher, J., Freibauer, A., 2011. Impact of tropical land-use change on soil

organic carbon stocks - a meta-analysis. Global Change Biol. 17, 1658–1670.
Dungait, J.A.J., Hopkins, D.W., Gregory, A.S., Whitmore, A.P., 2012. Soil organic matter turnover is governed by accessibility not recalcitrance. Global Change Biol. 18, 1781–1796.
Espirito-Santo, F.D.B., Gloor, M., Keller, M., Malhi, Y., Saatchi, S., Nelson, B., Oliveira, R.C., Pereira, C., Lloyd, J., Frolking, S., Palace, M., Shimabukuro, Y.E., Duarte, V., Mendoza, A.M., Lopez-Gonzalez, G., Baker, T.R., Feldpausch, T.R., Brienen, R.J.W., Asner, G.P., Boyd, D.S., Phillips, O.L., 2014. Size and frequency of natural forest disturbances and the amazon forest carbon balance. Nat. Commun. 5, 114–118.
Fang, C.M., Smith, P., Moncrieff, J.B., Smith, J.U., 2005. Similar response of labile and resistant soil organic matter pools to changes in temperature. Nature 433, 57–59.
Fang, J.Y., Liu, G.H., Zhu, B., Wang, X.K., Liu, S.H., 2007. Carbon budgets of three temperate forest ecosystems in Dongling Mt., Beijing, China. Sci. China Ser. D 50, 92–101.
FAO, 2006. Global Forest Resources Assessment 2005: Progress Towards Sustainable Forest Management. FAO, Rome, IT. Fao Forestry Paper 147.
Flores-Rentería, D., Rincón, A., Valladares, F., Curiel Yuste, J., 2016. Agricultural matrix affects differently the alpha and beta structural and functional diversity of soil microbial communities in a fragmented Mediterranean holm oak forest. Soil Biol. Biochem. 92, 79–90.
Fritze, H., Perkiomaki, J., Saarela, U., Katainen, R., Tikka, P., Yrjala, K., Karp, M., Haimi, J., Romantschuk, M., 2000. Effect of Cd-containing wood ash on the microflora of coniferous forest humus. FEMS Microbiol. Ecol. 32, 43–51.
Frostegard, A., Bååth, E., 1996. The use of phospholipid fatty acid analysis to estimate bacterial and fungal biomass in soil. Biol. Fert. Soils 22, 59–65.
Gamboa, A.M., Galicia, L., 2011. Differential influence of land use/cover change on topsoil carbon and microbial activity in low-latitude temperate forests. Agric. Ecosyst. Environ. 142, 280–290.
Garten, C.T., Post, W.M., Hanson, P.J., Cooper, L.W., 1999. Forest soil carbon inventories and dynamics along an elevation gradient in the southern Appalachian mountains. Biogeochemistry 45, 115–145.
Gershenson, A., Bader, N.E., Cheng, W.X., 2009. Effects of substrate availability on the temperature sensitivity of soil organic matter decomposition. Global Change Biol. 15, 176–183.
Goodale, C.L., Apps, M.J., Birdsey, R.A., Field, C.B., Heath, L.S., Houghton, R.A., Jenkins, J.C., Kohlmaier, G.H., Kurz, W., Liu, S.R., Nabuurs, G.J., Nilsson, S., Shvidenko, A.Z., 2002. Forest carbon sinks in the northern hemisphere. Ecol. Appl. 12, 891–899.
He, N.P., Yu, G.R., 2016. Stoichiometrical regulation of soil organic matter decomposition and its temperature sensitivity. Ecol. Evol. 6, 620–627.
He, N.P., Wang, R.M., Gao, Y., Dai, J.Z., Wen, X.F., Yu, G.R., 2013. Changes in the temperature sensitivity of SOM decomposition with grassland succession: implications for soil C sequestration. Ecol. Evol. 3, 5045–5054.
He, N.P., Wen, D., Zhu, J.X., Tang, X.L., Xu, L., Hu, H.F., Zhang, L., Huang, M., Yu, G.R., 2017. Vegetation carbon sequestration in Chinese forests from 2010 to 2050. Global Change Biol. 23, 1575–1584.
He, N.P., Tian, M., Liu, C.C., Li, M.L., Yang, H., Yu, G.R., Guo, D.L., Smith, M., Yu, Q., Hou, J.H., 2018. Variation in leaf anatomical traits from tropical to cold-temperate forests and linkage to ecosystem functions. Funct. Ecol. 32, 10–19.
Hong, S., Piao, S., Chen, A., Liu, Y., Liu, L., Peng, S., Sardans, J., Sun, Y., Penuelas, J., Zeng, H., 2018. Afforestation neutralizes soil pH. Nat. Commun. 9, 520.
Hooper, D., Coughlan, J., Mullen, M.R., 2008. Structural equation modeling: guidelines for determining model fit. Electron. J. Bus. Res. Methods 6, 141–146.
Huang, Y., Guenet, B., Ciais, P., Janssens, I.A., Soong, J.L., Wang, Y.L., Goll, D., Blagodatskaya, E., Huang, Y.Y., 2018. ORCHIMIC (v1.0), a microbe-driven model for soil organic matter decomposition designed for large-scale applications. Geosci. Model Dev. D 1–48. https://doi.org/10.5194/gmd-2017-325.
Iwai, C.B., Oo, A.N., Topark-Ngarm, B., 2012. Soil property and microbial activity in natural salt affected soils in an alternating wet–dry tropical climate. Geoderma 189-190, 144–152.
Kaiser, M., Kleber, M., Berhe, A.A., 2015. How air-drying and rewetting modify soil organic matter characteristics: an assessment to improve data interpretation and inference. Soil Biol. Biochem. 80, 324–340.
Lehmann, J., Kleber, M., 2015. The contentious nature of soil organic matter. Nature 528, 60–68.
Leifeld, J., von Lutzow, M., 2014. Chemical and microbial activation energies of soil organic matter decomposition. Biol. Fert. Soils 50, 147–153.
Li, J., He, N.P., Xu, L., Chai, H., Liu, Y., Wang, D.L., Wang, L., Wei, X.H., Xue, J.Y., Wen, X.F., Sun, X.M., 2017. Asymmetric responses of soil heterotrophic respiration to rising and decreasing temperatures. Soil Biol. Biochem. 106, 18–27.
Liu, Y., He, N.P., Zhu, J.X., Xu, L., Yu, G.R., Niu, S.L., Sun, X.M., Wen, X.F., 2017. Regional variation in the temperature sensitivity of soil organic matter decomposition in China's forests and grasslands. Global Change Biol. 23, 3393–3402. https://doi.org/10.1111/gcb.13613.
Liu, J., Jiang, P.K., Wang, H.L., Zhou, G.M., Wu, J.S., Yang, F., Qian, X.B., 2011. Seasonal soil CO_2 efflux dynamics after land use change from a natural forest to Moso bamboo plantations in subtropical China. Forest Ecol. Manag. 262, 1131–1137.
Lungo, A.D., Ball, J., Carle, J., 2006. Global Planted Forests Thematic Study: Results and Analysis. Planted Forests & Trees Working Papers.
Medlyn, B.E., Berbigier, P., Clement, R., Grelle, A., Loustau, D., Linder, S., Wingate, L., Jarvis, P.G., Sigurdsson, B.D., McMurtrie, R.E., 2005. Carbon balance of coniferous forests growing in contrasting climates: model-based analysis. Agric. For. Meteorol. 131, 97–124.
Min, K., Lehmeier, C.A., Ballantyne, F., Tatarko, A., Billings, S.A., 2014. Differential effects of pH on temperature sensitivity of organic carbon and nitrogen decay. Soil Biol. Biochem. 76, 193–200.
Niklinska, M., Klimek, B., 2007. Effect of temperature on the respiration rate of forest soil organic layer along an elevation gradient in the Polish Carpathians. Biol. Fert. Soils 43, 511–518.
Pries, C.E.H., Castanha, C., Porras, R.C., Torn, M.S., 2017. The whole-soil carbon flux in response to warming. Science 355, 1420–1422.
Saiya-Cork, K.R., Sinsabaugh, R.L., Zak, D.R., 2002. The effects of long term nitrogen deposition on extracellular enzyme activity in an Acer saccharum forest soil. Soil Biol. Biochem. 34, 1309–1315.
Schlesinger, W.H., Andrews, J.A., 2000. Soil respiration and the global carbon cycle. Biogeochemistry 48, 7–20.
Sharon, A.B., Ford, B.I., 2013. How interactions between microbial resource demands, soil organic matter stoichiometry, and substrate reactivity determine the direction and magnitude of soil respiratory responses to warming. Global Change Biol. 19, 90–102.
Shen, C., Xiong, J., Zhang, H., Feng, Y., Lin, X., Li, X., Liang, W., Chu, H., 2013. Soil pH drives the spatial distribution of bacterial communities along elevation on changbai mountain. Soil Biol. Biochem. 57, 204–211.
Sheng, H., Yang, Y.S., Yang, Z.J., Chen, G.S., Xie, J.S., Guo, J.F., Zou, S.Q., 2010. The dynamic response of soil respiration to land-use changes in subtropical China. Global Change Biol. 16, 1107–1121.
Shi, A.D., Marschner, P., 2014. Drying and rewetting frequency influences cumulative respiration and its distribution over time in two soils with contrasting management. Soil Biol. Biochem. 72, 172–179.
Shi, Z., Li, Y.Q., Wang, S.J., Wang, G.B., Ruan, H.H., He, R., Tang, Y.F., Zhang, Z.X., 2009. Accelerated soil CO2 efflux after conversion from secondary oak forest to pine plantation in southeastern China. Ecol. Res. 24, 1257–1265.
Shi, B.K., Gao, W.F., Jin, G.Z., 2015. Effects on rhizospheric and heterotrophic respiration of conversion from primary forest to secondary forest and plantations in northeast China. Eur. J. Soil Biol. 66, 11–18.
Sinsabaugh, R.L., Lauber, C.L., Weintraub, M.N., Ahmed, B., Allison, S.D., Crenshaw, C., Contosta, A.R., Cusack, D., Frey, S., Gallo, M.E., Gartner, T.B., Hobbie, S.E., Holland, K., Keeler, B.L., Powers, J.S., Stursova, M., Takacs-Vesbach, C., Waldrop, M.P., Wallenstein, M.D., Zak, D.R., Zeglin, L.H., 2008. Stoichiometry of soil enzyme activity at global scale. Ecol. Lett. 11, 1252–1264.
Smith, J.L., Halvorson, J.J., Hjr, B., 2002. Soil properties and microbial activity across a 500 m elevation gradient in a semi-arid environment. Soil Biol. Biochem. 34, 1749–1757.
Sochan, A., Bieganowski, A., Ryzak, M., Dobrowolski, R., Bartminski, P., 2012. Comparison of soil texture determined by two dispersion units of Mastersizer 2000. Int. Agrophys. 26, 99–102.
Sohng, J., Singhakumara, B.M.P., Ashton, M.S., 2017. Effects on soil chemistry of tropical deforestation for agriculture and subsequent reforestation with special reference to changes in carbon and nitrogen. Forest Ecol. Manag. 389, 331–340.
ter Braak, C.J.F., Smilauer, P., 2012. Canoco Reference Manual and User's Guide: Software for Ordination, Version 5.0. Microcomputer Power, Ithaca USA, pp. 2012.
Thiessen, S., Gleixner, G., Wutzler, T., Reichstein, M., 2013. Both priming and temperature sensitivity of soil organic matter decomposition depend on microbial biomass - an incubation study. Soil Biol. Biochem. 57, 739–748.
Tian, M., Yu, G.R., He, N.P., Hou, J.H., 2016a. Leaf morphological and anatomical traits from tropical to temperate coniferous forests: mechanisms and influencing factors. Sci. Rep. 6. https://doi.org/10.1038/srep19703.
Tian, Q.X., He, H.B., Cheng, W.X., Bai, Z., Wang, Y., Zhang, X.D., 2016b. Factors controlling soil organic carbon stability along a temperate forest altitudinal gradient. Sci. Rep. 6. https://doi.org/10.1038/srep18783.
Wang, Q., He, N.P., Liu, Y., Li, M.L., Xu, L., 2016a. Strong pulse effects of precipitation events on soil microbial respiration in temperate forests. Geoderma 275, 67–73.
Wang, Q., He, N.P., Yu, G.R., Gao, Y., Wen, X.F., Wang, R.F., Koerner, S.E., Yu, Q., 2016b. Soil microbial respiration rate and temperature sensitivity along a north-south forest transect in eastern China: patterns and influencing factors. J. Geophys. Res-Biogeo. 121, 399–410.
Wang, R.L., Yu, G.R., He, N.P., Wang, Q.F., Zhao, N., Xu, Z.W., 2016c. Latitudinal variation of leaf morphological traits from species to communities along a forest transect in eastern China. J. Geogr. Sci. 26, 15–26 (in Chinese).
Wieder, W.R., Grandy, A.S., Kallenbach, C.M., Taylor, P.G., Bonan, G.B., 2015. Representing life in the earth system with soil microbial functional traits in the MIMICS model. Geosci. Model Dev. 8, 1789–1808.
Xiong, J.B., Liu, Y.Q., Lin, X.G., Zhang, H.Y., Zeng, J., Hou, J.Z., Yang, Y.P., Yao, T.D., Knight, R., Chu, H.Y., 2012. Geographic distance and pH drive bacterial distribution in alkaline lake sediments across Tibetan plateau. Environ. Microbiol. 14, 2457–2466.
Xu, Z.W., Yu, G.R., Zhang, X.Y., Ge, J.P., He, N.P., Wang, Q.F., Wang, D., 2015. The variations in soil microbial communities, enzyme activities and their relationships with soil organic matter decomposition along the northern slope of Changbai Mountain. Appl. Soil Ecol. 86, 19–29.
Xu, W.F., Li, X.L., Liu, W., Li, L.H., Hou, L.Y., Shi, H.Q., Xia, J.Z., Liu, D., Zhang, H.C., Chen, Y., Cai, W.W., Fu, Y., Yuan, W.P., 2016. Spatial patterns of soil and ecosystem respiration regulated by biological and environmental variables along a precipitation gradient in semi-arid grasslands in China. Ecol. Res. 31, 505–513.
Xu, Z.W., Yu, G.R., Zhang, X.Y., He, N.P., Wang, Q.F., Wang, S.Z., Wang, R.L., Zhao, N., Jia, Y.L., Wang, C.Y., 2017. Soil enzyme activity and stoichiometry in forest ecosystems along the North-South Transect in eastern China (NSTEC). Soil Biol. Biochem. 104, 152–163.
Zhang, X.S., Yang, D.A., 1995. Eastern and northern transects of China research. Quaternary Sci. 01, 43–52 (in Chinese).
Zhang, Q., Wu, J.J., Yang, F., Lei, Y., Zhang, Q.F., Cheng, X.L., 2016. Alterations in soil microbial community composition and biomass following agricultural land use change. Sci. Rep. 6. https://doi.org/10.1038/srep36587.
Zhao, N., Yu, G.R., He, N.P., Wang, Q.F., Zhang, X.Y., Wang, R.L., Xu, Z.W., Jiao, C.C., Li, N.N., Jia, Y.L., 2016. Coordinated pattern of multi-element variability in the leaves and roots across Chinese forest biomes. Global Ecol. Biogeo. 25, 359–367.
Zhou, Z., Wang, C.K., Luo, Y.Q., 2018. Effects of forest degradation on microbial communities and soil carbon cycling: a global meta-analysis. Global Ecol. Biogeogr. 27, 110–124.